UCLA
UCLA Previously Published Works

Title

1,3-Dipolar Cycloaddition Reactivities of Perfluorinated Aryl Azides with Enamines and Strained Dipolarophiles

Permalink

https://escholarship.org/uc/item/5vd881rf

Journal

Journal of the American Chemical Society, 137(8)

ISSN

0002-7863

Authors

Xie, Sheng
Lopez, Steven A
Ramström, Olof
et al.

Publication Date

2015-03-04

DOI

10.1021/ja511457g

Peer reviewed

eScholarship.org Powered by the California Digital Library
University of California

Author Manuscript

Author Manuscript

Author Manuscript

Author Manuscript

HHS Public Access

Author manuscript

J Am Chem Soc. Author manuscript; available in PMC 2016 March 04.

Published in final edited form as:

J Am Chem Soc. 2015 March 4; 137(8): 2958–2966. doi:10.1021/ja511457g.

1,3-Dipolar Cycloaddition Reactivities of Perfluorinated Aryl Azides with Enamines and Strained Dipolarophiles

Sheng Xie[†,‡], **Steven A. Lopez**[∥,‡], **Olof Ramström**[*,†], **Mingdi Yan**[*,†,§], and **K. N. Houk**[*,∥]

[†]Department of Chemistry, KTH-Royal Institute of Technology, Teknikringen 36, Stockholm, Sweden

[§]Department of Chemistry, University of Massachusetts Lowell, Lowell, Massachusetts 01854, United States

[∥]Department of Chemistry and Biochemistry, University of California, Los Angeles, California 90095-1569, United States

Abstract

The reactivities of enamines and predistorted (strained) dipolarophiles toward perfluoroaryl azides (PFAAs) were explored experimentally and computationally. Kinetic analyses indicate that PFAAs undergo (3 + 2) cycloadditions with enamines up to 4 orders of magnitude faster than phenyl azide reacts with these dipolarophiles. DFT calculations were used to identify the origin of this rate acceleration. Orbital interactions between the cycloaddends are larger due to the relatively low-lying LUMO of PFAAs. The triazolines resulting from PFAA–enamine cycloadditions rearrange to amidines at room temperature, while (3 + 2) cycloadditions of enamines and phenyl azide yield stable, isolable triazolines. The 1,3-dipolar cycloadditions of norbornene and DIBAC also show increased reactivity toward PFAAs over phenyl azide but are slower than enamine–azide cycloadditions.

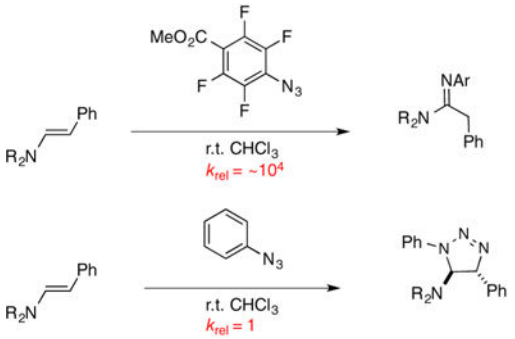

© XXXX American Chemical Society

Corresponding Authors mingdi_yan@uml.edu. houk@chem.ucla.edu. ramstrom@kth.se.
[‡]These authors contributed equally to this paper

Supporting Information

Experimental information, calculated geometries, and corresponding energies. This material is available free of charge via the Internet at http://pubs.acs.org.

Notes

The authors declare no competing financial interest.

Author Manuscript Author Manuscript Author Manuscript Author Manuscript

INTRODUCTION

Perfluorinated aryl azides (PFAAs) have been extensively utilized for the functionalization materials and surfaces[1] and for photoafinity labeling.[2] PFAAs are easily converted to nitrenes by photolysis or thermolysis. They are also relatively electrophilic due to the presence of strongly electronegative fluorine atoms. PFAAs have been further used as photocoupling agents, primarily by the Yan group, to functionalize surfaces and nanomaterials[3] and are relatively stable to elevated temperatures (Table S1, Supporting Information). Here we report a theoretical and experimental exploration of the 1,3-dipolar cycloadditions of PFAAs to expand the reagents that can be used for surface functionalization of enamines and strained dipolarophiles such as norbornene and dibenzoazacyclooctyne (DIBAC).

Huisgen discovered 1,3-dipolar cycloadditions of azides in the 1960s.[4] Meldal and Sharpless independently developed the click reaction of azides and terminal alkynes that requires Cu catalysis to form triazoles efficiently and regioselectively,[5,6] resulting in renewed interest in the cycloaddition.[7] Azide–alkyne cycloadditions, particularly those involving strained alkynes, now constitute a key bioorthogonal reaction used to label biomolecules in vivo.[8] Initial calculations on 1,3-dipolar cycloadditions of PFAAs predicted that these electron-deficient aryl azides would undergo rapid cycloadditions with electronrich dipolarophiles such as enamines. We explored substituent effects on several aryl azides with various *p*-electron-with-drawing groups (EWGs) (**a–f**) in cycloadditions to enamines (**1–8**), norbornene (**9**), and DIBAC (**10**) (Scheme 1). The rates for these cycloadditions are compared to those for ambiphilic azides **g** and **h**.

RESULTS AND DISCUSSION

The rate constants for these 1,3-dipolar cycloadditions were determined in $CDCl_3$ with a 2:1 ratio of azide to dipolarophile. Most reactions were monitored by ^1H NMR or ^{19}F NMR spectroscopy, and the second-order rate constants (k_c) were found based on the triazoline or triazole formation rate. Detailed information about the kinetic studies we performed can be found in the Experimental Section and Supporting Information.

Acetophenone-Derived Enamine Cycloadditions

The reaction of acetophenone enamines and PFAAs gave perfluoroanilines as the major products (60–90% isolated yields) on the basis of ^{19}F and ^1H NMR spectroscopy (Figure S1A, Supporting Information). These triazolines decomposed to perfluoroanilines by a mechanism that is not known with certainty (Scheme 2).[9]

The k_c for the cycloadditions of azides to enamine **1** were determined using ^{19}F NMR (**a–c, f**) or ^1H NMR (**g** and **h**) and are shown in Table 1. These data are presented as a plot of triazoline concentration vs time in the Supporting Information.

Author Manuscript Author Manuscript Author Manuscript Author Manuscript

Phenylacetaldehyde-Derived Enamine Cycloadditions

Scheme 3 shows the 1,3-dipolar cycloadditions of **a–f** to enamines (**5–8**) under ambient conditions. Intermediate triazolines bearing a perfluoroaryl group underwent a room-temperature rearrangement (observed by ^{1}H and ^{19}F NMR) to afford amidines (Scheme 3).

Figure 1 shows the scope of these reactions and experimental yields. The triazolines were only transiently observed as intermediates by ^{1}H and ^{19}F NMR.

We show the first example of fluorinated aryl azides that undergo (3 + 2) cycloadditions at room temperature to afford amidines. Triazolines bearing electron-deficient aryl groups are known to decompose, and several mechanisms have been proposed for this rearrangement.[10] Erba and co-workers recently performed DFT calculations on the rearrangement mechanism.[11] We are currently exploring in more detail how N_2 is extruded from triazolines to afford amidines.

Table 2 gives k_c and the corresponding experimental activation free energies ($\Delta G^{\ddagger}_{exp}$). Rate constants for cyclo-additions were found in the same manner as for reactions of acetophenone-derived enamines. However, triazolines [(**a–g**)-(**5–8**)] decompose to form amidines [(**a–g**)-(**5–8**)]′.

The rate constants for the cycloadditions of **5–8** and aryl azides (**a-h**) are summarized in Table 2. The reactivities of PFAAs with phenylacetaldehyde-derived enamines follow the same trend as that of acetophenone-derived enamines but have k_c that are 5–10-fold greater, likely due to of the greater steric bulk associated with ketonic enamines. The reaction between a and **5** is nearly 4 orders of magnitude faster than that of phenyl azide. The rate constant for the cycloaddition of 4-nitroperfluorophenyl azide (**d**) and **5** is 1.216 ± 0.032 M^{-1} s^{-1}, which is the fastest for the cycloaddition of an azide with an unstrained dipolarophile. The mechanism of 1,3-dipolar cycloadditions involving enamines and phenyl azide has been explored experimentally by Munk[12] and computationally by Houk.[13] The rate constants of the cycloaddition between PFAA (**a, b**) and enamine (**5−8**) were subsequently measured and are summarized in Table 3.

The reactivities of enamines toward PFAAs decrease in the following order: **7, 5, 6**. Munk et al. observed the same trend experimentally for the reactions of phenyl azide with the same substrates.[13a] Lopez and Houk showed that the reactions of PhN_3 and enamines are concerted and proceed through relatively asynchronous transition structures.[13] The asynchronicity of the reactions arises from a strong orbital interaction of the high-lying enamine HOMO with the LUMOs of phenyl azide and to a greater extent with the PFAAs studied here. Computationally, both concerted and stepwise mechanisms were considered; the transitions structures for both modes of cycloaddition are shown in Figure 2.

The activation free energies for the stepwise cycloadditions are greater than the $\Delta G^{\ddagger}$ of the corresponding concerted reaction by 5−7 kcal mol^{-1} and will not be considered further. In comparison to experimental $\Delta G^{\ddagger}$ (Table 2), computed activation free energies for concerted cycloaddition are greater by 1−3 kcal mol^{-1}. However, the qualitative reactivity trends observed experimentally are reproduced computationally.

Author Manuscript Author Manuscript Author Manuscript Author Manuscript

Figure 2 shows that the activation free energies decrease for the transition structures involving increasingly electron-deficient aryl azides along the series **TS-g5, TS-b5**, and **TS-a5** ($\Delta G^{\ddagger}$ = 25.3, 21.7, and 21.0, respectively). These transition structures are concerted but asynchronous. The transition structures have bond lengths between the *β*-carbon and the terminal azide nitrogen (C*β*-N) that are more developed than the other forming bond (C*α*–N). The (C_{α}–N) forming bond lengths (ca. 2.6 Å) are nearly unchanged in these transition structures. The C_{β}−N forming bond lengths are also similar in **TS-a5** and **TS-b5** (ca. 2.1 Å). This forming bond is notably shorter in **TS-g5**, 2.04 Å.

We utilized the distortion/interaction model[14] to understand the origins of the reactivity difference of PFAAs studied experimentally with enamines and strained dipolarophiles. The activation energy ($\Delta E^{\ddagger}$) is dissected into distortion energy ($\Delta E^{\ddagger}_{d}$) and interaction energy (ΔE_{i}). Distortion energy is the energy required to distort each of the reactants into their respective transition state geometries, without allowing the fragments to interact. The interaction energy is the energy of interaction between the distorted cycloaddends. It is often a net stabilizing quantity that results from charge transfer of occupied–vacant orbital interactions, electrostatic interactions, polarization, and closed-shell (steric) repulsions. Figure 3 summarizes our findings as a graph of $\Delta E^{\ddagger}$, ΔE_{d} (enamine), $\Delta E^{\ddagger}_{d}$ (azide), and ΔE_{i} for **TS-a5, TS-b5**, and **TS-g5**.

The graph in Figure 3 suggests that **TS-g5** has the highest activation energy because of increased total cylcoaddend distortion and reduced interaction between the dipole and the dipolarophile. Both components of distortion energy (green and blue) increase from left to right in Figure 3. **TS-g5** occurs latest, which means that the cycloaddends are most distorted from their reactant geometries. A frontier molecular orbital (FMO) analysis can be used to understand how interaction energies contribute to the activation energies of these reactions. Figure 4 shows the computed molecular orbitals of enamine 5 and azides **a, b**, and **g**.

The major stabilizing orbital interaction is between the HOMO of enamine **5** and the LUMO of **a, b**, and **g**. Perfluorination of the phenyl ring substantially lowers the azide LUMO energies of **a** and **b**, resulting in smaller HOMO− LUMO gaps and stronger FMO interactions.

1,3-Dipolar Cycloadditions of Norbornene and PFAAs

Motivated by the use of strained alkenes in bioorthogonal reactions, we explored the reactivity of norbornene toward PFAAs (**a−c, f**), phenyl azide (**g**), and benzyl azide (**h**) (Scheme 4). Additions to norbornene are fast and *exo* stereoselective. At 25 °C, PFAAs react with norbornene faster than does phenyl azide. Rate constants for these reactions are summarized in Table 4.

Representative transition structures **TS-a9, TS-b9**, and **TS-g9** are shown in Figure 5. The transition structures are concerted but slightly asynchronous. The bond length between the carbon and the terminal azide nitrogen ($C–N_{term}$) is slightly shorter than that of the carbon and internal nitrogen ($C−N_{int}$) for each of these transition structures.

Author Manuscript Author Manuscript Author Manuscript Author Manuscript

The $\Delta E^{\ddagger}$ of **TS-a9** and **TS-b9** are lower in energy (11.5 and 11.7 kcal mol^{-1}, respectively) than **TS-9g** (14.4 kcal mol^{-1}). The higher $\Delta E^{\ddagger}$ for PhN_3 cycloadditions arise from increased distortion energies and less favorable interaction energies. The $\Delta E^{\ddagger}$ of **TS-a9** and **TS-b9** are nearly identical (22.2 and 22.3 kcal mol^{-1}) and increase to 23.6 kcal mol^{-1} in **TS-g9**. The newly forming bonds in **TS-g9** are more developed than **TS-a9** or **TS-b9**, which requires additional distortion of the cycloaddends to reach the geometries of the transition structures. The interaction energies are more favorable for **TS-a9** and **TS-b9** (−10.7 and −10.6, respectively) than **TS-g9** (−9.2 kcal mol^{-1}). The dominant FMO interaction is that of the LUMO of dipole and the relatively high-lying HOMO (ca. −7.79 eV) of norbornene. The reactions with the greatest interaction energies involve the most electrophilic dipole, azide a.

Reactivity Enhancement by Predistortion vs Orbital Effects

Perfluorophenyl azide reacts with enamine 5 25-fold faster than norbornene (9) (k_c = 1.05 × 10^{-2} and 4.08 × 10^{-4} M^{-1} s^{-1}, respectively). The distortion/interaction model was used to understand why orbital effects outweigh norbornene predistortion. The $\Delta E^{\ddagger}$ for **TS-b5** and **TS-b9** are 7.4 and 11.7 kcal mol^{-1}, respectively; the distortion energies are 26.1 and 22.3 kcal mol^{-1}, respectively. The double bond of norbornene is pyramidalized and resembles the exo transition structure (i.e., the reaction is distortion accelerated).[13a] The interaction energies for **TS-b5** and **TS-b9** are −18.7 and −10.6 kcal mol^{-1}, respectively. The HOMO of norbornene is not as high lying as 5, and does not interact strongly with the LUMO of b. The enhanced interaction energy component overrides norbornene predistortion.

Cycloadditions of DIBAC

In addition to examining norbornene as a dipolarophile in these cycloadditions, the cycloaddition of PFAAs with other predistorted dipolarophiles, including benzocyclooctynes bioorthogonal reagents like DIBAC,[15] DIBO,[16] DIFO,[17] and BARAC, were explored. These strained alkynes are used as bioorthogonal probes to label cell–surface azido glycans (Scheme 5).

BARAC shows the greatest reactivity toward benzyl azide cycloadditions (0.96 M^{-1} s^{-1}).[18] Computations by the Houk group have explained how predistortion and substituent effects control the reactivities of BARAC and its derivatives.[19] Here we performed cycloadditions of PFAAs, phenyl, and benzyl azide to DIBAC (**10**, Scheme 6). Experimental observations using ^{1}H and ^{19}F NMR for product **a-10** (Figure S32, Supporting Information) indicated a mixture of regioisomers in a ratio of 1:0.4. Attempts to assign the identity of the isomers however proved inconclusive. Rate constants were measured and are shown in Table 5.

DIBAC is more reactive with PFAAs than with PhN_3 and shows poor regioselectivity. We use the M06-2X density functional to understand the differences in reactivity of aryl azides with 10 used model dibenzoazacyclooctyne, 11. The global minimum of 11 is shown in Figure 7.

As expected, the amide isomerization is facile at room temperature. We computed 12 possible transition structures (differing in *syn/anti* orientation of azide and *s-trans/s-cis* amide conformation and three conformations of the aryl ring for the reaction of **a, b**, and **g**

Author Manuscript Author Manuscript Author Manuscript Author Manuscript

with **11** (see Supporting Information for higher energy transition structures). Table 6 shows the activation free energies for the regioisomeric transition structures for the reactions of azides **a, b**, and **g** to **11**. The lowest energy transition structures for the *syn* and *anti* approaches of the azide [**TS(g11-*syn*)** and **TS(g11-*anti*)**] are shown in Figure 8.

These transition structures are almost perfectly synchronous. The C−N bond lengths range only from 2.19 to 2.24 Å. While computations do not quantitatively reproduce experimental activation free energies, the experimental reactivity trends are reproduced by theory. Our calculations show that the $\Delta G^{\ddagger}$ for **TS(a11-syn)** and **TS(b11-syn)** are lower in energy than the corresponding anti transition states by 0.7 and 0.6 kcal mol^{-1}, respectively. These results suggest that there should be a small preference for the syn regioisomers for PFAAs. The $\Delta G^{\ddagger}$ for **TS(g11-*syn*)** and **TS(g11-*anti*)** are identical, which should result in a 1:1 mixture of *syn* and *anti* regioisomers.

To understand why PFAAs are more reactive than phenyl azide in cycloadditions involving DIBAC, distortion/interaction analyses were performed on **TS(a11-*syn*)**, **TS(b11-*syn*)**, and **TS(g11-*syn*)** (Figure 9).

The interaction energies are nearly constant, and the distortion energies control the small difference in reactivities.

CONCLUSION

We experimentally and computationally explored the 1,3-dipolar cycloaddition of PFAAs to enamines and strained dipolarophiles (norbornene and DIBAC). Perfluorination of phenyl group of these aryl azides accelerates cycloadditions to all of the substrates studied here. This is due to improved orbital interactions with the relatively low-lying LUMO of PFAAs. Despite the predistortion of norbornene, PFAAs prefer to react with enamines because of the much more favorable interaction energies. These cycloadditions give triazolines as intermediates that rearrange at room temperature to give amidines, while cycloadditions involving enamines and phenyl azide yield isolable triazolines. The mechanism of triazoline decomposition is currently being investigated.

EXPERIMENTAL METHODS

Materials

Azides, ketonic enamines, and aldehydic enamines were synthesized using reported procedures.[20,21] All compounds were stored at −20 °C, and compound purity was assessed by ^{1}H NMR before performing kinetic studies. Norbornene (bicyclo[2.2.1]hept-2-ene, 99%) and DIBAC (dibenzocyclooctyneamine, >94.5%) were purchased from Sigma-Aldrich and used as received. In kinetic studies, $CDCl_3$ was filtered through K_2CO_3 and treated over molecular sieves. The amount of water in the purified $CDCl_3$ was 0.3 ppm, measured by a 756 KF Coulometer, which was <1 mol % enamines used in all kinetic studies.

Author Manuscript Author Manuscript Author Manuscript Author Manuscript

Cycloaddition Reaction between Azide and Enamine (Schemes 2 and 3)

The following describes the reaction between PFPA a and enamine 5. Other reactions were carried out using the same protocols. To a solution of 5 (1.0 mmol) in THF (1.0 mL) a solution of a (1.1 mmol) in THF (1.0 mL) was added dropwise while stirring at room temperature. Reaction progress was monitored by NMR spectroscopy. Upon a reaction's completion (8−12 h), the solvent was removed under reduced pressure and the residual mixture was purified by flash column chromatography (hexanes/EtOAc = 9:1, R_f = 0.27) yielding (a-5)′ as a white powder (390 mg, 95%). Alternatively, the reactions could be carried out in methanol (1.5−3 mL) using a slight excess of enamines (1.1 equiv). In this case, the amidine product precipitated out from the solution within 12 h and the product was separated by filtration (isolated yields > 70% for all amidines).

Cycloaddition between Azide and Norbornene (Scheme 4)

The following describes the reaction of azide c with norbornene 9. Reactions of other azides followed the same protocol. To a solution of norbornene 9 (1.25 mmol) in hexanes (2−4 mL), azide c (1.00 mmol) was added. The solution was set at room temperature without stirring until a white solid started to form. When TLC indicated full conversion of the azide, the mixture was cooled to −20 °C and filtered and the solid was washed with a small amount of hexanes to afford the product as a white solid (270 mg, 87%).

Cycloaddition Reaction between Azide and DIBAC

In a typical reaction, a solution of DIBAC in $CDCl_3$ (9.0 mM) was added into a solution of azide (18 mM). The reactions were followed by NMR. The products were not isolated and only characterized by NMR as presented in the kinetic studies.

Kinetic Studies

Kinetic experiments were conducted using NMR following similar protocols reported in the literature.[12,15,19] In a typical experiment, a solution of azide in deuterated solvent was mixed with an equal volume of the dipolarophile in an NMR tube at a mole ratio of 2:1. ^1H or ^{19}F NMR spectra of the sample were recorded on a Bruker AVANCE (400 or 500 MHz) spectrometer every 1.5−5 min. The acquisition time for a typical experiment was 30 s for ^1H NMR and 18 s for ^{19}F NMR. In the ^1H NMR studies, the peaks of the dipolarophile were monitored, which decreased as the reaction proceeded. In the ^{19}F NMR studies, the F signals in PFPAs and the cycloaddition products were followed. Each reaction was allowed to proceed to 10−90% conversion. Every experiment was repeated at least three times.

To calculate the rate constant of the cycloaddition reaction, the conversion−time curve was constructed. The curves were then fit to the standard second-order kinetic model using the statistic software GraphPad prism (see Supporting Information for detailed calculations). The characteristic peaks of the intermediates and products can be found in corresponding datasheets in the Supporting Information.

Author Manuscript Author Manuscript Author Manuscript Author Manuscript

COMPUTATIONAL METHODS

All computations were carried out with Gaussian 09.[22] Reactants, transition states, and products were optimized with the density functional M06-2X[23] using the 6-31G(d) basis set with an ultrafine grid, consisting of 590 radial shell and 99 grid points per shell.[24] M06-2X has been found to give reliable energetics for cycloadditions involving main group elements.[25] Normal vibrational mode analysis confirmed all stationary points to be minima (no imaginary frequencies) or transition states (one imaginary frequency). Zero-point energy and thermal corrections were computed from unscaled frequencies for the standard state of 1 M and 298.15 K. Truhlar's quasiharmonic correction was applied for entropy calculations by setting all frequencies less than 100 cm^{-1} to 100 cm^{-1}.[26,27] Input structures for these computations were generated using Gaussview.

Supplementary Material

Refer to Web version on PubMed Central for supplementary material.

ACKNOWLEDGMENTS

We thank the National Science Foundation (NSF CHE-1059084 to K.N.H. and CHE-1112436 to M.Y.) and KTH for financial support of this research. S.L. thanks Dr. Colin Lam, Rob Giacometti, and Ashay Patel for helpful discussions. S.X. thanks the China Scholarship Council for a special scholarship award. Calculations were performed on the Hoffman2 cluster at UCLA and the Extreme Science and Engineering Discovery Environment (XSEDE), which is supported by National Science Foundation grant number OCI-10535. Figures 2, 5, 7, and 8 were generated using CYLview.[28]

REFERENCES

1. (a) Cai S, Nabity JC, Wybourne MN, Keana JFW. Chem. Mater. 1990; 2:631.(b) Yan M, Cai S, Wybourne MN, Keana JFW. Chem. Mater. 1994; 5:151.(c) Yan M, Cai S, Keana JFW. J. Org. Chem. 1994; 59:5951.(d) Yan M, Ren J. Chem. Mater. 2004; 16:1627.(e) Joester D, Klein E, Geiger B, Addadi L. J. Am. Chem. Soc. 2006; 128:1119. [PubMed: 16433527]
2. (a) Schnapp KA, Poe R, Leyva E, Soundararajan N, Platz MS. Bioconjugate Chem. 1993; 4:172.(b) Kapfer I, Jacques P, Toubal H, Goeldner MP. Bioconjugate Chem. 1995; 6:109.(c) Tate JJ, Persinger J, Bartholomew B. Nucleic Acids Res. 1998; 26:1421. [PubMed: 9490787] (d) Baruah H, Puthenveetil S, Choi YA, Shah S, Ting AY. Angew. Chem., Int. Ed. 2008; 47:7018.(e) Jung ME, Chamberlain BT, Ho CL, Gillespie EJ, Bradley KA. ACS. Med. Chem. Lett. 2014; 5:363. [PubMed: 24900841]
3. (a) Liu LH, Yan M. Acc. Chem. Res. 2010; 43:1434. [PubMed: 20690606] (b) Pastine SJ, Okawa D, Kessler B, Rolandi M, Llorente M, Zettl A, Frechet JM. J. Am. Chem. Soc. 2008; 130:4238. [PubMed: 18331043] (c) Park J, Yan M. Acc. Chem. Res. 2013; 46:181. [PubMed: 23116448] (d) Chen X, Ramström O, Yan M. Nano. Res. 2014; 7:1381.
4. Huisgen R. Angew. Chem., Int. Ed. 1963; 2:565.
5. (a) Rostovtsev VV, Green LG, Fokin VV, Sharpless KB. Angew. Chem., Int. Ed. 2002; 41:2596.(b) Agnew HD, Rohde RD, Millward SW, Nag A, Yeo WS, Hein JE, Pitram SM, Tariq AA, Burns VM, Krom RJ, Fokin VV, Sharpless KB, Heath JR. Angew. Chem., Int. Ed. 2009; 48:4944.
6. Tornøe CW, Christensen C, Meldal M. J. Org. Chem. 2002; 67:3057. [PubMed: 11975567]
7. Brase S, Gil C, Knepper K, Zimmermann V. Angew. Chem., Int. Ed. 2005; 44:5188.
8. (a) Sletten EM, Bertozzi CR. Angew. Chem., Int. Ed. 2009; 48:6974.(b) Bertozzi CR. Acc. Chem. Res. 2011; 44:651. [PubMed: 21928847]
9. The decomposition of the triazolines was furthermore accompanied by a rapid color change from light yellow to dark red as well as the evolution of gas after 20−60 min reaction time

Author Manuscript Author Manuscript Author Manuscript Author Manuscript

10. (a) Fusco R, Bianchetti G, Pocar D. Gazz. Chim. Ital. 1961; 91:933.(b) Fusco R, Bianchetti G, Pocar D, Ugo R. Chem. Ber. 1963; 96:802.(c) Shea KJ, Kim J-S. J. Am. Chem. Soc. 1992; 114:4846.
11. Contini A, Erba E. RSC. Adv. 2012; 2:10652.
12. Meilahn MK, Cox B, Munk ME. J. Org. Chem. 1975; 40:819.
13. (a) Lopez SA, Munk ME, Houk KN. J. Org. Chem. 2013; 78:1576. [PubMed: 23347077] (b) Jones GO, Houk KN. J. Org. Chem. 2008; 73:1333. [PubMed: 18211089]
14. Ess DH, Houk KN. J. Am. Chem. Soc. 2007; 129:10646. [PubMed: 17685614]
15. Debets MF, van Berkel SS, Schoffelen S, Rutjes FP, van Hest JC, van Delft FL. Chem. Commun. 2010; 46:97.
16. Ning X, Guo J, Wolfert MA, Boons G-J. Angew. Chem., Int. Ed. 2008; 47:2253.
17. Baskin JM, Prescher JA, Laughlin ST, Agard NJ, Chang PV, Miller IA, Lo A, Codelli JA, Bertozzi CR. Proc. Natl. Acad. Sci. U.S.A. 2007; 104:16793. [PubMed: 17942682]
18. Jewett JC, Sletten EM, Bertozzi CR. J. Am. Chem. Soc. 2010; 132:3688. [PubMed: 20187640]
19. Gordon CG, Mackey JL, Jewett JC, Sletten EM, Houk KN, Bertozzi CR. J. Am. Chem. Soc. 2012; 134:9199. [PubMed: 22553995]
20. (a) Keana JFW, Cai SX. J. Org. Chem. 1990; 55:3640.(b) Chapyshev SV. Chem. Heterocycl. Compd. 2001; 37:968–975.(c) Berger O, Kaniti A, van Ba C, Vial H, Ward S, Biagini G, Bray P, O'Neill P. ChemMedChem. 2011; 6:2094. [PubMed: 21905228] (d) Serwinski P, Esat B, Lahti P, Liao Y, Walton R, Lan JJ. Org. Chem. 2004; 69:5247.(e) Jin LM, Xu X, Lu H, Cui X, Wojtas L, Zhang XP. Angew. Chem., Int. Ed. 2013; 52:5309.
21. (a) Carlson R, Nilsson Å , ; Carlström K, Skoldefors H, Wilking N, Theve N. Acta Chem. Scand. B. 1984; 38:49.(b) Amat M, Canto M, Llor N, Escolano C, Molins E, Espinosa E, Bosch J. J. Org. Chem. 2002; 67:5343. [PubMed: 12126426]
22. Frisch, MJ.; Trucks, GW.; Schlegel, HB.; Scuseria, GE.; Robb, MA.; Cheeseman, JR.; Scalmani, G.; Barone, V.; Mennucci, B.; Petersson, GA.; Nakatsuji, H.; Caricato, M.; Li, X.; Hratchian, HP.; Izmaylov, AF.; Bloino, J.; Zheng, G.; Sonnenberg, JL.; Hada, M.; Ehara, M.; Toyota, K.; Fukuda, R.; Hasegawa, J.; Ishida, M.; Nakajima, T.; Honda, Y.; Kitao, O.; Nakai, H.; Vreven, T.; Montgomery, JA., Jr.; Peralta, JE.; Ogliaro, F.; Bearpark, M.; Heyd, JJ.; Brothers, E.; Kudin, KN.; Staroverov, VN.; Kobayashi, R.; Normand, J.; Raghavachari, K.; Rendell, A.; Burant, JC.; Iyengar, SS.; Tomasi, J.; Cossi, M.; Rega, N.; Millam, JM.; Klene, M.; Knox, JE.; Cross, JB.; Bakken, V.; Adamo, C.; Jaramillo, J.; Gomperts, R.; Stratmann, RE.; Yazyev, O.; Austin, AJ.; Cammi, R.; Pomelli, C.; Ochterski, JW.; Martin, RL.; Morokuma, K.; Zakrzewski, VG.; Voth, GA.; Salvador, P.; Dannenberg, JJ.; Dapprich, S.; Daniels, AD.; Farkas, O.; Foresman, JB.; Ortiz, JV.; Cioslowski, J.; Fox, DJ. Gaussian 09, revision C.01. Gaussian, Inc.; Wallingford, CT: 2010.
23. Zhao Y, Truhlar DG. Theor. Chem. Acc. 2008; 120:215.
24. Wheeler SE, Houk KN. J. Chem. Theory Comput. 2010; 6:395. [PubMed: 20305831]
25. Zhao Y, Truhlar DG. Acc. Chem. Res. 2008; 41:157. [PubMed: 18186612]
26. Zhao Y, Truhlar DG. Phys. Chem. Chem. Phys. 2008; 10:2813. [PubMed: 18464998]
27. Ribeiro RF, Marenich AV, Cramer CJ, Truhlar DG. J. Phys. Chem. B. 2011; 115:14556. [PubMed: 21875126]
28. Legault, CY. CYLview 1.0b. Universite de Sherbrooke; Sherbrooke: 2014. www.cylview.org)

Author Manuscript Author Manuscript Author Manuscript Author Manuscript

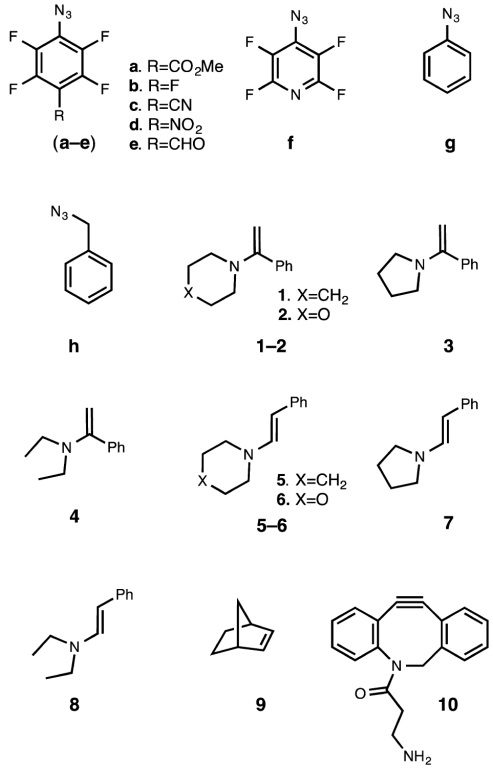

Scheme 1.

Azide and Dipolarophile Scope for the (3 + 2) Cycloadditions Studied Here

Author Manuscript Author Manuscript Author Manuscript Author Manuscript

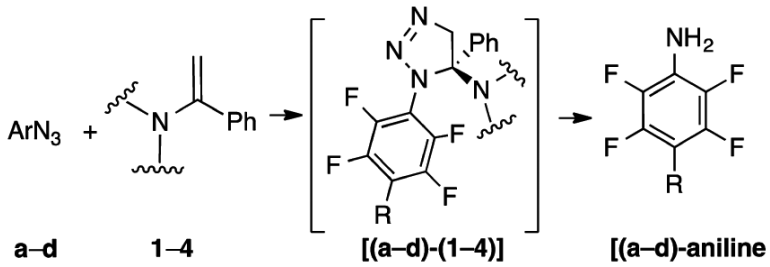

Scheme 2.
Cycloadditions of PFAAs and Acetophenone Enamines

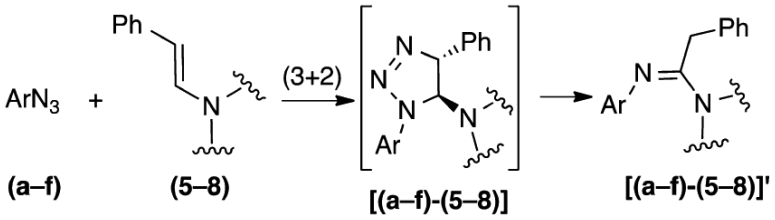

Scheme 3.

Reaction of PFAAs (**a–f**) and Phenylacetaldehyde Enamines (**5–8**) Result in Triazolines [(a–f)-(5–8)] that Lose N_2 To Form Amidines

Author Manuscript Author Manuscript Author Manuscript Author Manuscript

Author Manuscript Author Manuscript Author Manuscript Author Manuscript

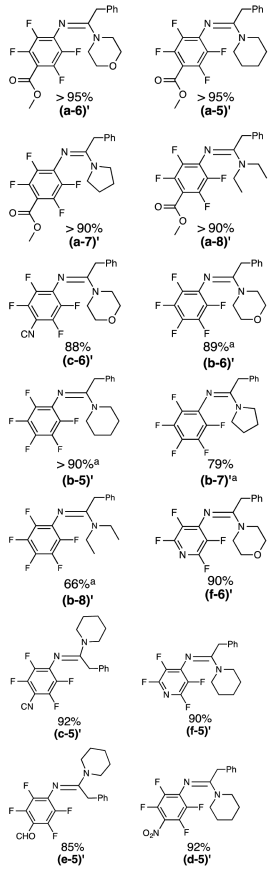

Figure 1.

Amidines isolated experimentally. Reaction conditions: enamine (1.0 mmol), azide (1.1 mmol), THF or MeOH (2 mL), room temperature. Isolated yields after 12 h. (a) After 72 h. When decomposition was incomplete, the yield was calculated against the conversion of the enamine reactant.

Author Manuscript Author Manuscript Author Manuscript Author Manuscript

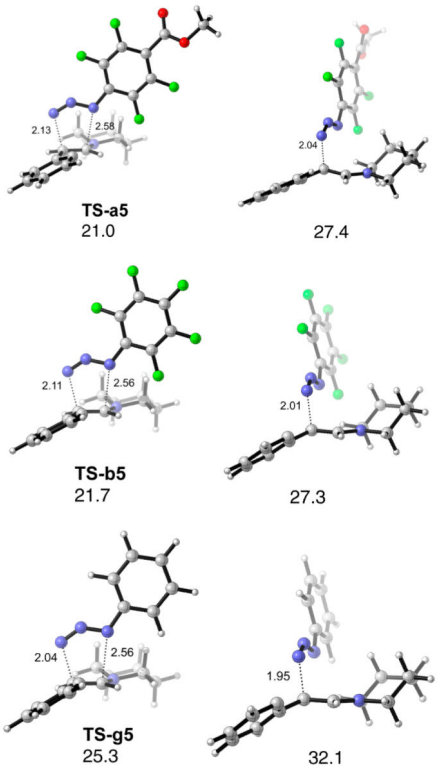

Figure 2.

Concerted transition structures for the (3 + 2) cycloaddition of PFAAs (a and b) and phenyl azide (g) to 5 are in the left column. Stepwise transition structures are in the right column. Computed using M06-2X/6-311+G(d,p)/IEFPCM^{CGCl3}//M06-2X/6-31G(d)/IEFPCM^{CHCl3}. Bond lengths are reported in Angstroms, and reported energies are Gibbs free energies in kcal mol^{-1} determined assuming a standard state of 1 M and 298.15 K.

Author Manuscript Author Manuscript Author Manuscript Author Manuscript

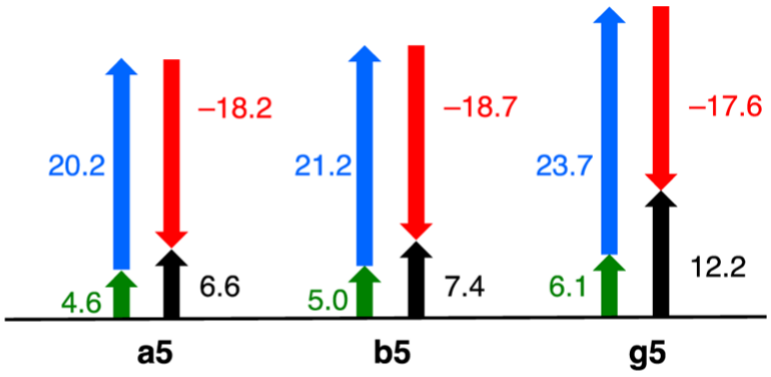

Figure 3.

Graph of activation, distortion, and interaction energies for **TS-a5**, **TS-b5**, and **TS-g5** (black, activation energies; green, distortion energies of dipolarophile; blue, distortion energies of azides; red, interaction energies). Calculated using M06-2X/6-311+G(d,p)/IEFPCM^{CHCl3}//M06-2X/6-31G(d)/IEFPCM^{CHCl3}.

Author Manuscript Author Manuscript Author Manuscript Author Manuscript

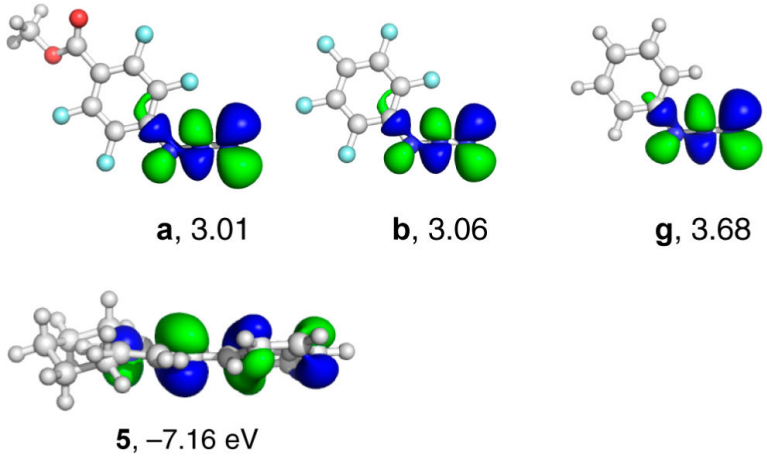

Figure 4.

Computed LUMOs of azides **a, b**, and **g** and the HOMO of enamine 5. Orbital energies are reported in eV and calculated using HF/6-31G(d)//M06-2X/6-31G(d)/IEF-PCM^{CHCl3}.

Author Manuscript Author Manuscript Author Manuscript Author Manuscript

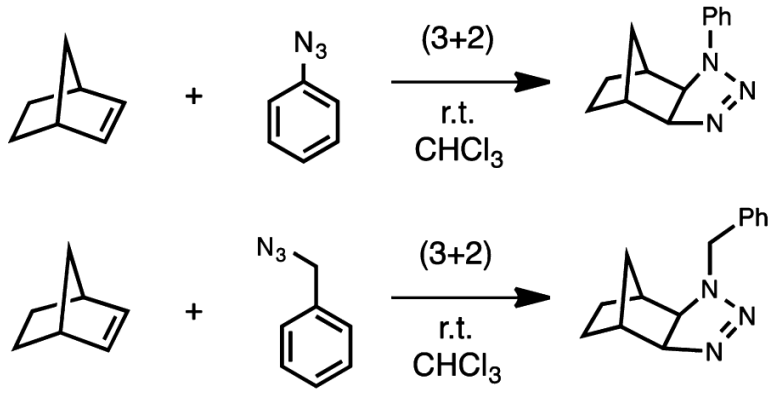

Scheme 4.

(3 + 2) Cycloadditions of Phenyl and Benzyl Azides to Norbornene

Author Manuscript Author Manuscript Author Manuscript Author Manuscript

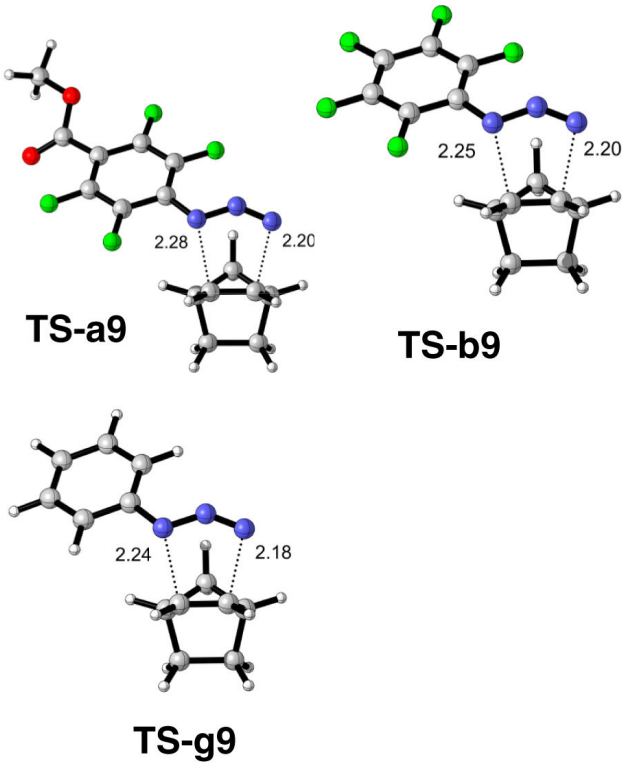

Figure 5.

Transition structures for the (3 + 2) cycloadditions of norbornene (**9**) and **a, b**, and **g**. Computed using M06-2X/6311+G(d,p)/IEFPCM^{CHCl3}//M06-2X/31G(d)/IEFPCM^{CHCl3}.

Author Manuscript Author Manuscript Author Manuscript Author Manuscript

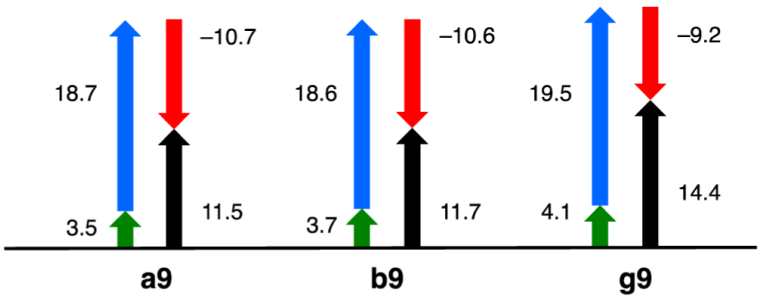

Figure 6.

Graph of activation, distortion, and interaction energies for **TS-a9**, **TS-b9**, and **TS-g9** (black, activation energies; green, distortion energies of dipolarophile; blue, distortion energies of azides; red, interaction energies). Calculated using M06-2X/6-311+G(d,p)/IEFPCM^{CHCl3}//M06-2X/6-31G(d)/IEF-PCM^{CHCl3}.

Author Manuscript Author Manuscript Author Manuscript Author Manuscript

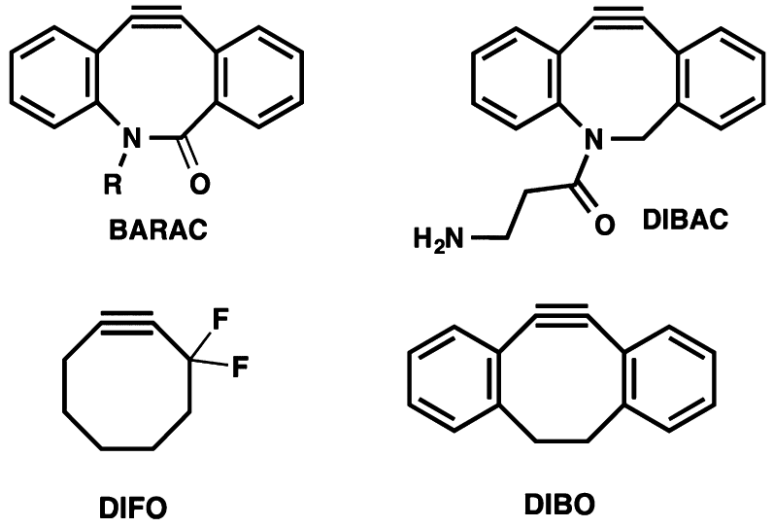

Scheme 5.

Some Cyclooctynes DIBO, DIBAC, DIFO, and DIBO Known To Participate in Bioorthogonal Reactions

Author Manuscript Author Manuscript Author Manuscript Author Manuscript

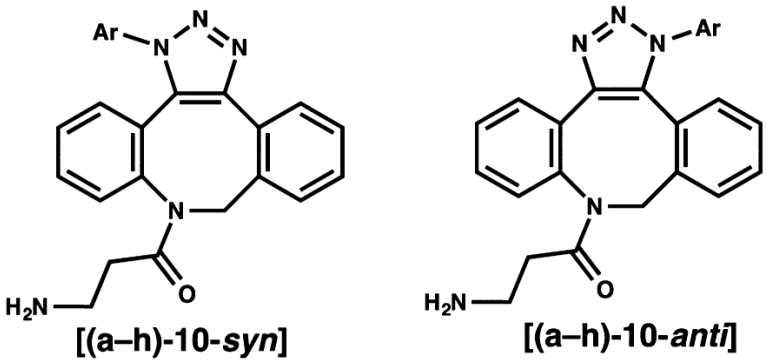

Scheme 6.

Regioisomeric Products Resulting from the Reaction of 10 with Azides (a, b, or g)

Author Manuscript Author Manuscript Author Manuscript Author Manuscript

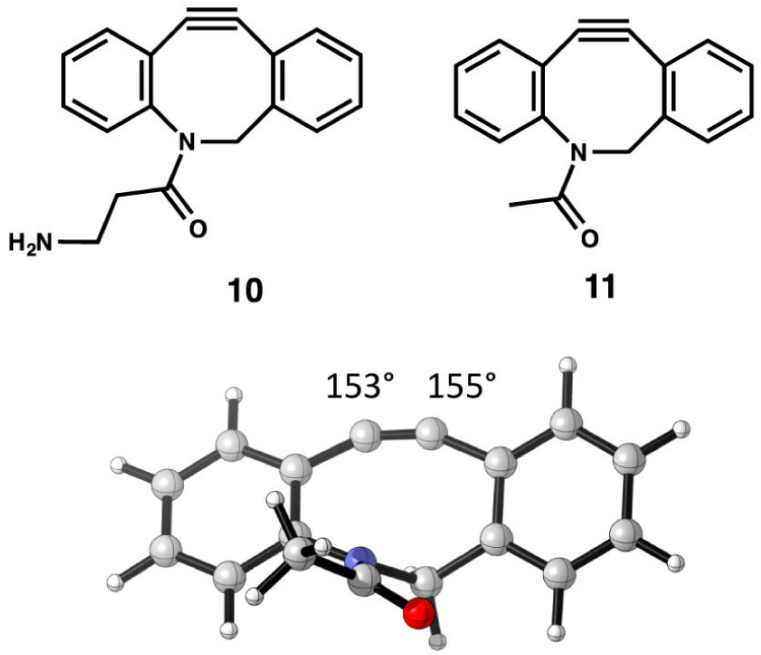

Figure 7.
Lowest energy conformer of dibenzocyclooctyne **11**. Alkyne bond angles are reported in degrees.

Author Manuscript Author Manuscript Author Manuscript Author Manuscript

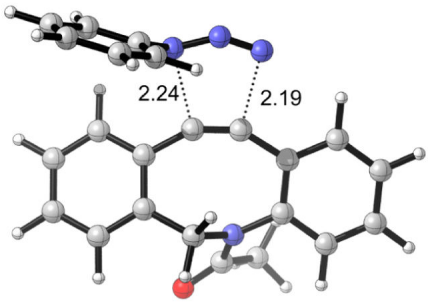

TS(g11-*syn*)

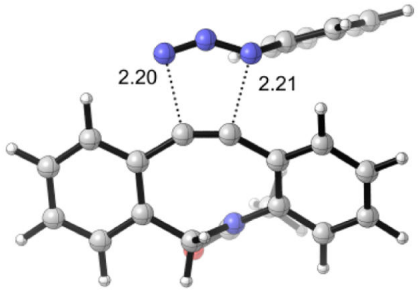

TS(g11-*anti*)

Figure 8.

Lowest energy syn and anti transition structures for cycloadditions of **g** to **11**. Bond lengths are reported in Angstroms and energies in kcal mol^{-1}. Computed free energies in solution are for the standard state of 1 M and 298.15 K using M06-2X/6-311+G(d,p)/IEFPCM^{CHCl3}// M06-2X/6-31G(d)/IEFPCM^{CHCl3}.

Author Manuscript Author Manuscript Author Manuscript Author Manuscript

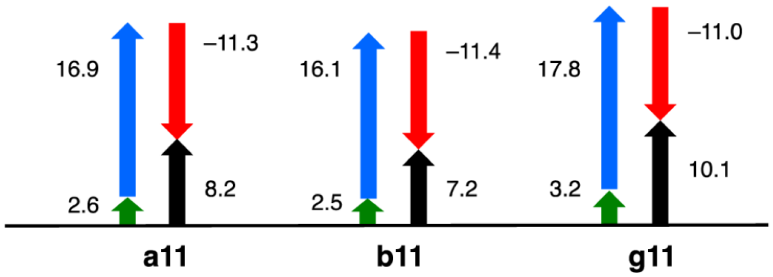

Figure 9.

Graph of activation, distortion, and interaction energies for **TS-a11**, **TS-b11**, and **TS-g11** (black, activation energies; green, distortion energies of dipolarophile; blue, distortion energies of azides; red, interaction energies). Calculated using M06-2X/6-311+G(d,p)/IEFPCM^{CHCl3}//M06-2X/6-31G(d)/IEFPCM^{CHCl3}.

Author Manuscript

Author Manuscript

Author Manuscript

Author Manuscript

Table 1

Rate Constants (k_c) for the (3 + 2) Cycloadditions of (a–d, g, and h) to 1[a]

Azide	k_c (10^{-2} M^{-1} s^{-1})	k_{rel}[b]	$\Delta G^{\ddagger}_{exp}$[c] (kcal mol^{-1})
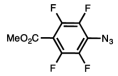 **a**	1.41 ± 0.04	16,300	20.0 ± 0.1
b	0.126 ± 0.05	1,450	21.0 ± 0.1
c	11.8 ± 0.06	135,000	18.4 ± 0.1
f	15.9 ± 0.4	185,000	18.2 ± 0.1
g	0.867 ± 0.04 x 10^{-4}	1	25.3 ± 0.1
h	n.d.	–	–

[a]Conditions: [Azide]:[Enamine] 2:1, ^1H and ^{19}F NMR in $CDCl_3$, 293.0 K, Figures S2–S6, Supporting Information. [b]$k_{rel} = k_c(\mathbf{a–h})/k_c(\mathbf{g})$. [c]Calculated from the Eyring equation ($k_B = 1$).

Author Manuscript Author Manuscript Author Manuscript Author Manuscript

Table 2

Rate Constants (k_c) for the (3 + 2) Cycloadditions of Azides (a–h) and Phenylacetaldehyde Piperidine Enamine 5[a]

Azide	k_c (10^{-2} M^{-1} s^{-1})	k_{rel}[b]	$\Delta G^{\ddagger}_{exp}$[c] (kcal mol^{-1})
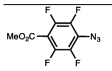 **a**	7.22 ± 0.04	9,080	18.7 ± 0.1
b	1.05 ± 0.03	1,320	19.8 ± 0.1
c	97.2 ± 2.4	122,000	17.2 ± 0.1
d	121.6 ± 3.2	153,000	17.0 ± 0.1
e	35.9 ± 0.6	45,000	17.7 ± 0.1
f	80.8 ± 0.2	102,000	17.3 ± 0.1
g	1.85 x 10^{-3} ± 0.02	1	24.0 ± 0.1[d]
h	< 10^{-5} [f]	–	–

[a]Conditions: [Azide]:[Enamine] 2:1, ^1H and ^{19}F NMR in $CDCl_3$, 293.0 K, Figures S7–S13, Supporting Information. [b]$k_{rel} = k_c(\mathbf{a–h})/k_c(\mathbf{g})$, at 293.0 K. [c]Calculated from the Eyring equation ($k_B = 1$) . [d]At 298.0 K.

Author Manuscript

Author Manuscript

Author Manuscript

Author Manuscript

Table 3

Constants of the Cycloadditions of a and b with 5–8[a]

Enamine	k_c (**a**) (10^{-2} M^{-1} s^{-1})	k_c (**b**) (10^{-2} M^{-1} s^{-1})
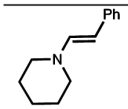 **5**	7.22 ± 0.04 (11)	1.05 ± 0.03 (11)
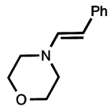 **6**	0.639 ± 0.001 (1)	0.098 ± 0.002 (1)
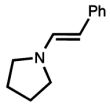 **7**	17.6 ± 0.2 (27)	2.29 ± 0.06 (23)
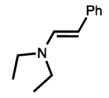 **8**	10.1 ± 0.1 (16)	1.35 ± 0.03 (14)

[a]Rates were determined by ^1H and ^{19}F NMR in $CDCl_3$, [Azide]:[Enamine] 2:1, 293.0 K, Figures S14–S19, Supporting Information. Relative rate constants are given in parentheses.

Author Manuscript Author Manuscript Author Manuscript Author Manuscript

Table 4

Azid–Norbornene (3 + 2) Cycloaddition Rate Constants and Corresponding Activation Free Energies[a]

Azide	k_c (10^{-4} M^{-1} s^{-1})	k_{rel}[b]	$\Delta G^{\ddagger}$[c] (kcal mol^{-1})
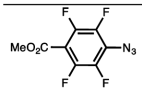 **a**	9.13 ± 0.06	60	21.3 ± 0.1
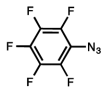 **b**	4.08 ± 0.03	27	21.8 ± 0.1
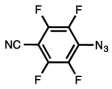 **c**	28.0 ± 0.2	185	20.7 ± 0.1
f	30.9 ± 0.2	205	20.6 ± 0.1
g	0.151 ± 0.022	1	23.7 ± 0.1
h	0.0184 ± 0.002	0.12	25.0 ± 0.1

[a]Conditions: [Azide]:[Norbornene] 2:1, ^1H and ^{19}F NMR in $CDCl_3$, 294.7 K, Figures S20–S25, Supporting Information. [b]$k_{rel} = k_c(\mathbf{a}–\mathbf{h})/k_c(\mathbf{g})$. [c]Calculated from the Eyring equation ($k_B = 1$) .

Author Manuscript Author Manuscript Author Manuscript Author Manuscript

Table 5

Azide–DIBAC (10) Cycloaddition Rate Constants and Corresponding Activation Free Energies[a]

Azide	k_c (10^{-2} M^{-1} s^{-1})	k_{rel}[b]	$\Delta G^{\ddagger}$[c] (kcal mol^{-1})
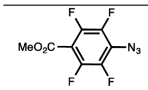 **a**	4.88 ± 0.11	1.96	19.0 ± 0.1
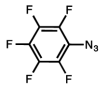 **b**	11.1 ± 0.4	4.45	18.5 ± 0.1
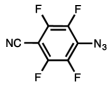 **c**	4.28 ± 0.1	1.72	19.1 ± 0.1
f	2.58 ± 0.05	1.03	19.4 ± 0.1
g	2.49 ± 0.03	1	19.4 ± 0.1
h	21.9 ± 0.3	8.8	18.1 ± 0.1

[a]Conditions: [Azide]:[DIBAC] 2:1, ^1H or ^{19}F NMR in $CDCl_3$, 294.7 K. Figures S26–S31, Supporting Information. [b]k_{rel}: relative rate $k_c/k_c(\mathbf{g})$. [c]Calculated from the Eyring equation (k_B = 1).

Author Manuscript Author Manuscript Author Manuscript Author Manuscript

Table 6

Activation Free Energies for the Cycloadditions Involving a, b, and g to 11[a]

Azide	$\Delta G_{syn}^{\ddagger}$	$\Delta G_{anti}^{\ddagger}$
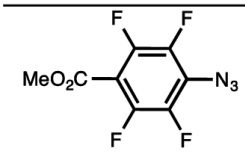 **a**	23.4	24.1
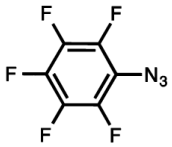 **b**	22.2	22.8
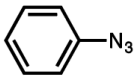 **g**	24.0	24.0

[a]Activation free energies are reported in kcal mol^{-1}. Computed free energies in solution are for the standard state of 1 M and 298.15 K.